CCC Annual Report

UIUC, August 19, 2015

Argon Bubble Behavior in EMBr Field

Kai Jin

Department of Mechanical Science & Engineering

University of Illinois at Urbana-Champaign

Introduction

- Argon bubbles are commonly injected during Continuous Casting (CC) process, and understanding the motion of such argon bubbles is important (e.g. inclusion removal by bubble flotation[1])
- Transverse magnetic field changes bubble dynamics
- This work studies motion of a single argon gas bubble rising in quiescent liquid steel with an external magnetic field (EMBr)
- Volume-of-Fluid (VOF) method with reduced spurious velocities was implemented into CUFLOW, validated and used
- Results from this study will be used to improve the Lagrangian nozzle-mold model by modifying the drag force in particle transport equations

Dimensionless Numbers

- Bubble Reynolds number $Re_b = \rho_l \sqrt{gd}\, d\, \mu_l^{-1}$
- Terminal Reynolds number $Re_\tau = \rho_l u_\tau d \mu_l^{-1}$
- Eötvös number $Eo = \left(\rho_l - \rho_g\right) g d^2 \gamma^{-1}$
- Bond number $Bo = \rho_l g d^2 \gamma^{-1}$
- Morton number (material property) $Mo = g \mu_l^4 \left(\rho_l - \rho_g\right) \rho_l^{-2} \gamma^{-3}$
- Laplace number $La = \mu_l^{-2} \sigma \rho L$
- Hartmann number $Ha = Bd\sqrt{(\sigma / \mu)}$
- Stuart number $N = Ha^2 Re_b^{-1}$

d – bubble diameter; ρ – density; μ – viscosity;
g – gravity acceleration; γ – bubble-liquid interfacial tension;
B – magnetic field strength; σ – fluid electrical conductivity.
subscripts l and g denote liquid and gas, respectively

Governing Equations

- Continuity $\nabla \cdot \left(\rho \mathbf{u}\right) = 0$
- Momentum $\rho \dfrac{\partial \mathbf{u}}{\partial t} + \rho\left(\mathbf{u} \cdot \nabla\right)\mathbf{u} = -\nabla p + \nabla \cdot \left[\mu\left(\nabla \mathbf{u} + \nabla \mathbf{u}^T\right)\right] + \mathbf{F}_L + \mathbf{F}_S + \rho \mathbf{g}$
- Volume fraction $\dfrac{\partial \alpha}{\partial t} + \mathbf{u} \cdot \nabla \alpha = 0$

$\boldsymbol{u}$ is mixture velocity, t is time, ρ is mixture density, μ is mixture dynamic viscosity, p is total pressure and $\boldsymbol{g}$ is gravity, α volume fraction of steel. Source terms: $\boldsymbol{F}_L$ - Lorentz force and $\boldsymbol{F}_S$ - surface tension force

- MHD equations

$$\mathbf{J} = \sigma\left(-\nabla \Phi + \mathbf{u} \times \mathbf{B}\right) \qquad \nabla \cdot \mathbf{J} = 0$$

$$\nabla \cdot \left(\sigma \nabla \Phi\right) = \nabla \cdot \left[\sigma\left(\mathbf{u} \times \mathbf{B}\right)\right] \qquad \mathbf{F}_L = \mathbf{J} \times \mathbf{B}$$

- Surface tension force

$$\mathbf{F}_S = \int_\Gamma \gamma \kappa \mathbf{n} \delta\left(\mathbf{x} - \mathbf{x}_f\right) \mathrm{ds}$$

κ is the mean interface curvature, Γ represents the interface, $\mathbf{n}$ is the normal vector of the interface, δ is the Dirac delta function. Solve the dimensionless equations, with scale: μ_l, ρ_l, $(gd)^{1/2}$ as velocity scale, $(g/d)^{1/2}$ as time scale

Solution Method

- Use in-house multi-GPU code, CUFLOW to solve equations
- Integrate three-dimensional unsteady incompressible Navier-Stokes equations on multiple Cartesian grids
- Solve continuity and momentum equations using fractional step method
- Three Poisson equations (pressure-Poisson equation, electrical-Poisson equation and surface-tension related Poisson equation) are solved efficiently on a GPU with a V-cycle multigrid method, and red-black SOR with over-relaxation parameter of 1.6

Spurious Velocity Reduction in VOF
(P. Kumar, UIUC, 2015)

- A Sharp Surface Force (SSF) method for modeling of the surface tension force was adapted into CUFLOW when using VOF [3,4]
- Demonstrate method on test problem: static air bubble in water with no gravity. Results: spurious velocities arising with traditional VOF method in low-Morton number systems are mainly avoided.

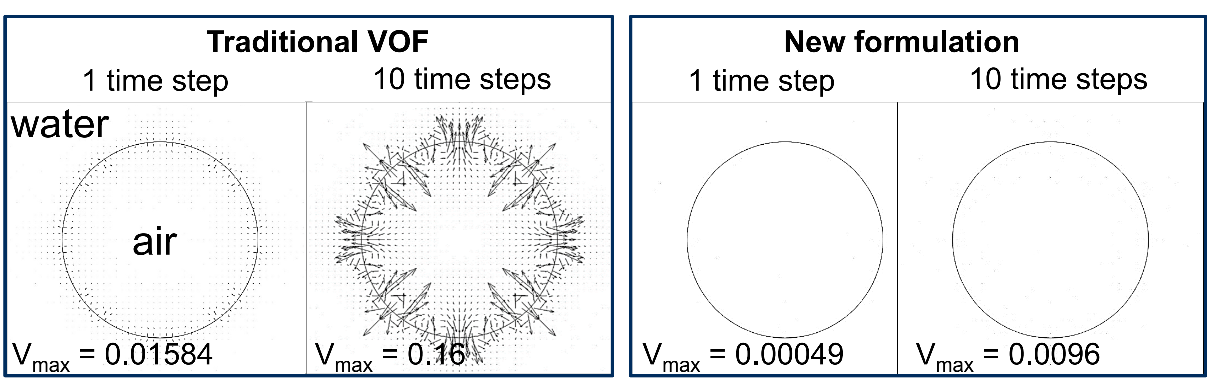

32 cells across bubble diameter.

Validation – Air Bubble Rise in Water

- Both air-water and argon-steel systems have similar numerical challenge (large density ratio and low Morton number), but many measurements are available for comparison in air-water system.
- Six validation simulations were conducted for air bubbles rising in water.
- Release single bubble (1mm ≤ d ≤ 7mm), from bottom of tall, square water tank (4d × 4d ×10d in rising direction).

TABLE I: Properties of air and water, argon and steel

	Air	Water	Argon	Steel
T (K)	300		1773	
γ (N/m)	0.0712		1.2	
ρ (kg/m3)	1.17	1000	0.56	7000
μ (kg/(m·s))	1.86×10^{-5}	0.001	7.42×10^{-5}	0.0063
σ (1/(Ω·s))	1.00×10^{-15}	0.001	1.00×10^{-15}	714000

TABLE II: Dimensionless numbers of air-water and Ar-steel (d = 3 mm)

	Eo	Mo	Re_b	ρ_l/ρ_g	μ_l/μ_g	σ_l/σ_g
air-water	1.24	2.7×10^{-11}	514.4	8.547×10^{2}	53.8	1.0×10^{12}
argon-steel	0.51	1.3×10^{-12}	571.5	1.250×10^{4}	84.3	7.4×10^{20}

Validation Results – Predicted Terminal Velocity and Bubble Shape

- Compare with published experimental and computational results
- More details can be found elsewhere [4]

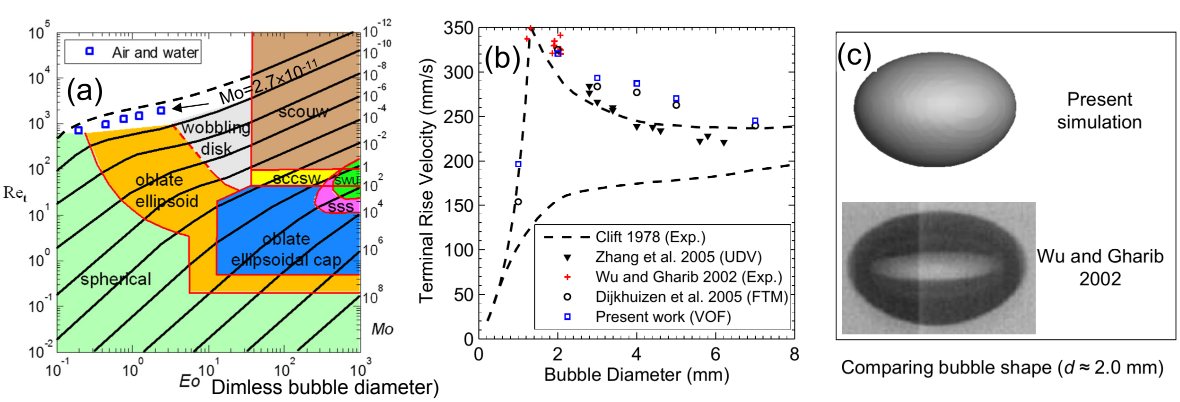

Comparing bubble shape ($d \approx 2.0$ mm)

(a) Eo vs. predicted Re_T on Grace diagram. Bubble shape: scouw - spherical cap with open unsteady wake; sccsw - spherical cap with closed steady wake; swu - with wavy unsteady skirt; sss – with smooth steady skirt [5, 6]
(b) Comparison of predicted terminal velocities of bubbles of different size
(c) Predicted shape of a 2 mm bubble after rising ~6.7 mm

List of Simulations

- Total 6 simulations solved using BlueWaters super computer
  - 2 different bubble diameters: 3 and 7 mm
  - 3 different magnetic field strengths: 0, 0.2 and 0.5 Tesla
- Magnetic field ***B*** along *x* direction
- All walls no slip and no penetration
- Walls are eclectically insulated
- Grid independence study[2] shows 32 cells cross bubble is enough, ~19 millions cells in domain

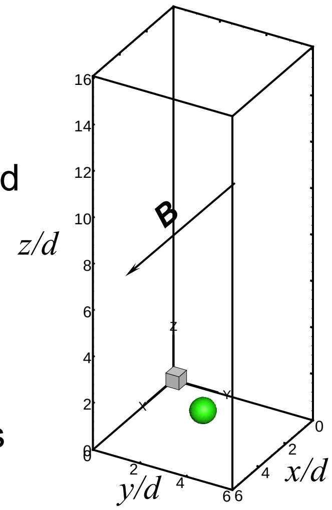

TABLE III: Simulations of Ar bubble rising in liquid steel (Mo = 1.3 × 10^{-12}, 1773 K)

d(mm)	Eo	Re_b	No.	B(T)	Ha	N	No.	B(T)	Ha	N	No.	B(T)	Ha	N
3	0.51	572	1	0.0	0.00	0.00	2	0.2	6.39	0.07	3	0.5	15.97	0.45
7	2.80	2037	4	0.0	0.00	0.00	5	0.2	14.90	0.11	6	0.5	37.26	0.68

Animation of Bubble & Vorticity Magnitude |Ω*| Isosurface

3mm B=0T **3mm B=0.2T** **7mm B=0T** **7mm B=0.2T**

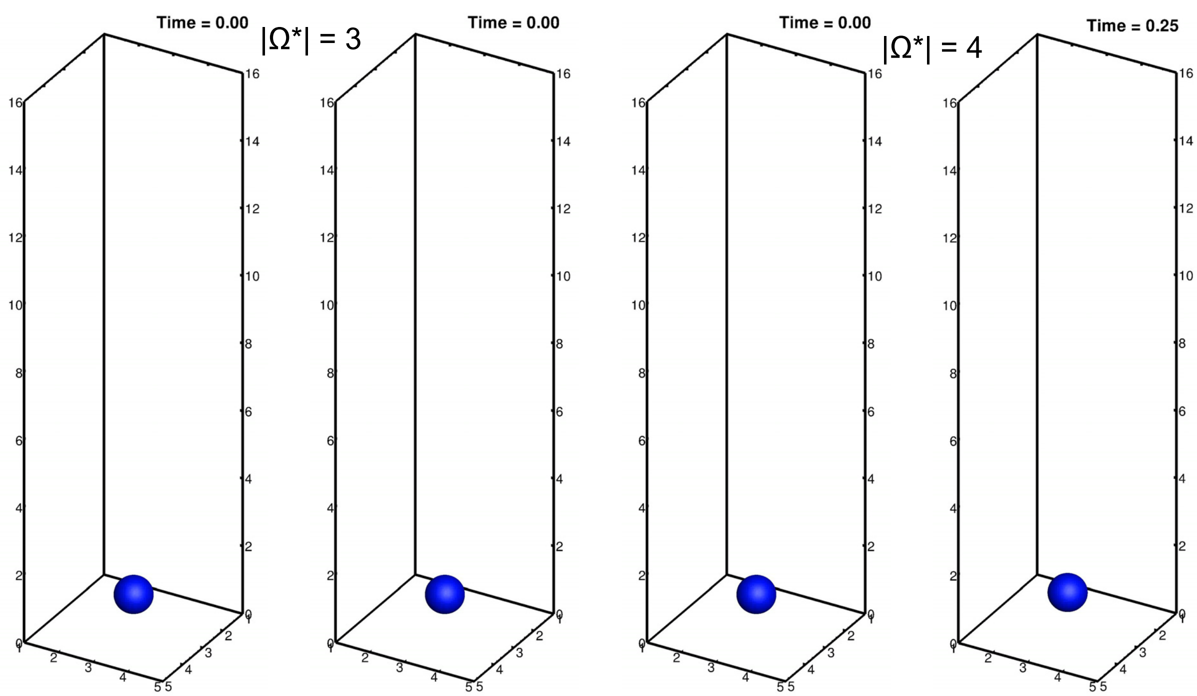

Wake behind the 3mm Bubble (Isosurface of Vorticity Magnitude)

- Front and side views of the isosurface of vorticity magnitude $|\Omega^*|=3$ at t=0.1s for different B, 3mm bubble

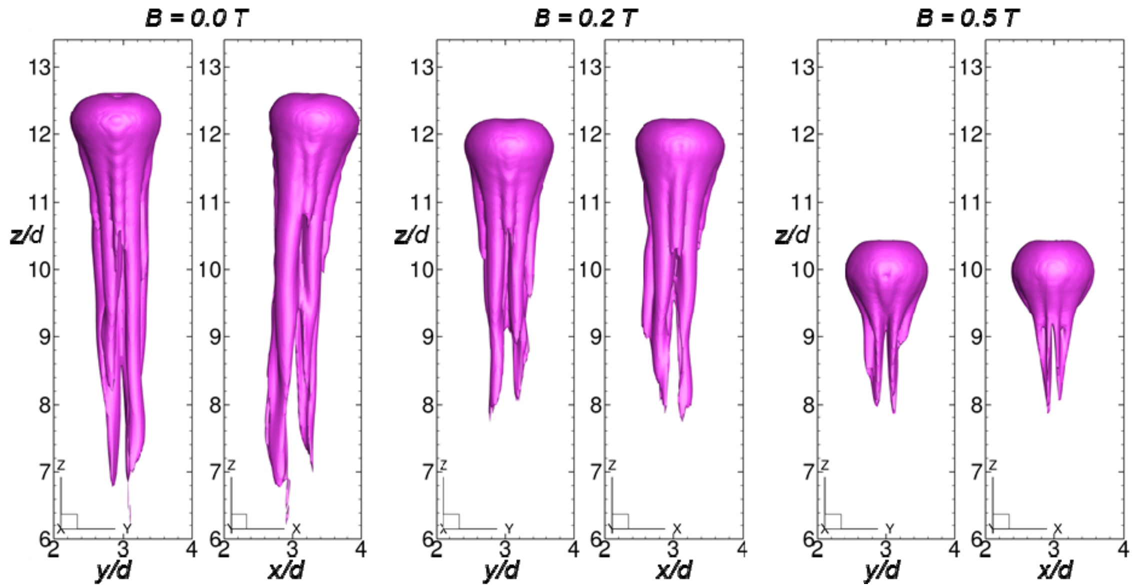

Wake behind the 7mm Bubble (Isosurface of Vorticity Magnitude)

- Front and side views of the isosurface of vorticity magnitude $|\Omega^*|=4$ at t=0.24s for different B, 7mm bubble

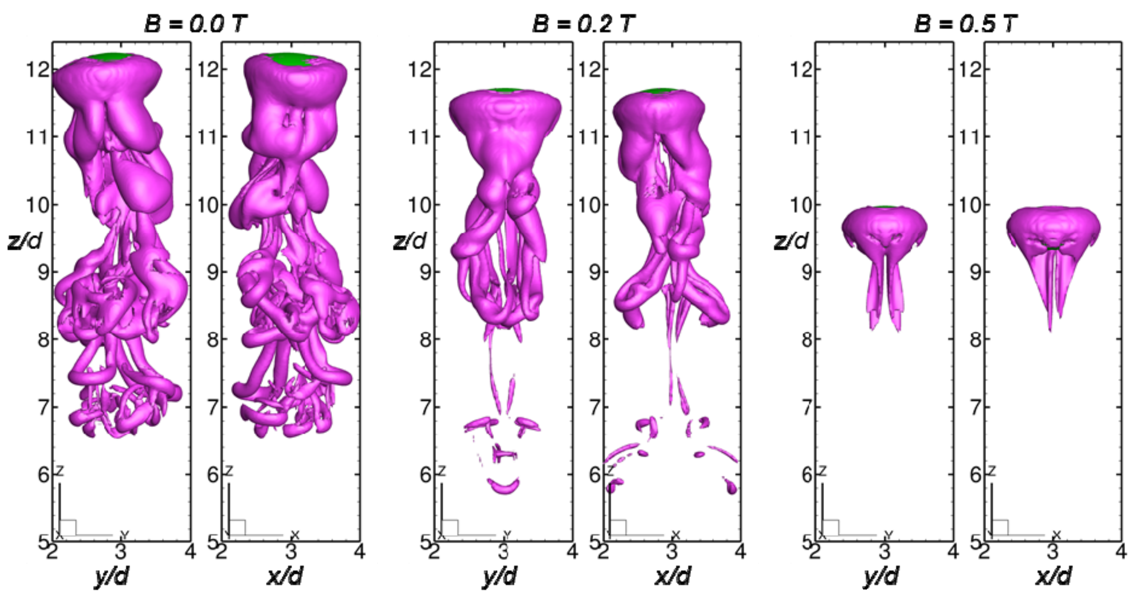

Continuous Casting Consortium

Animation of Z Vorticity $\Omega^*_z = \pm 1$

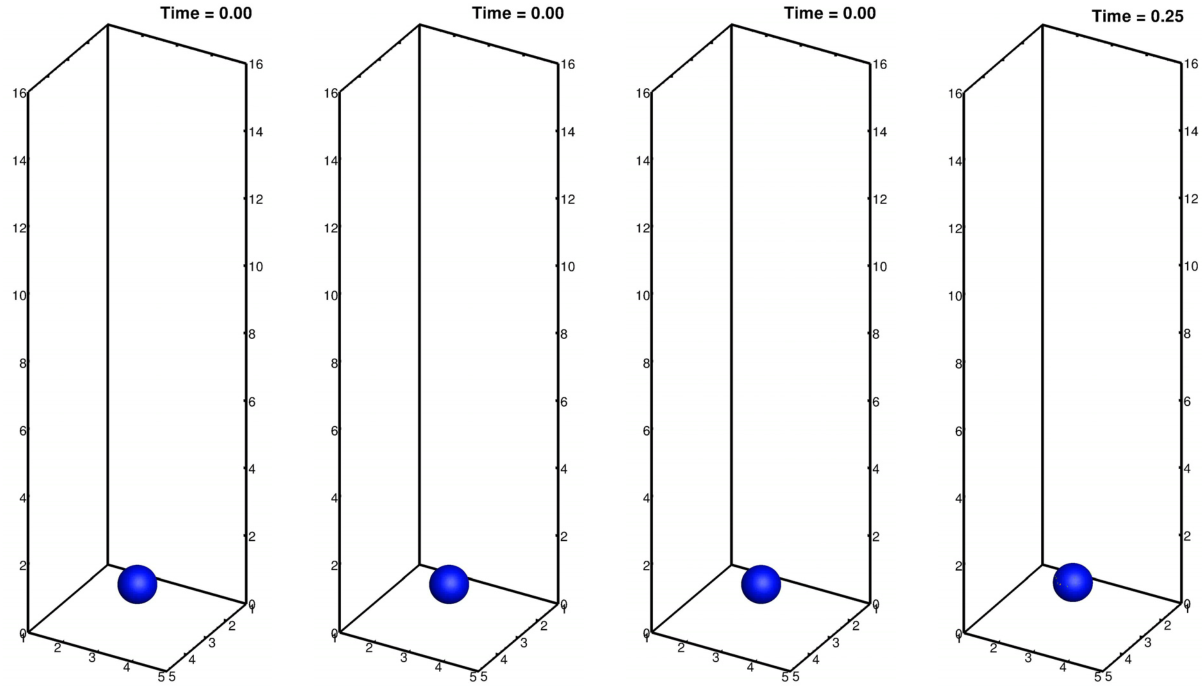

Continuous Casting Consortium

Wake behind the 3mm Bubble (Z Vorticity)

- Front and side views, isosurfaces of $\Omega^*_z = \pm 1$ at t=0.1s, 3mm bubble
- Ω^*_z alternates in sign → fluid in z direction has alternating rotation pairs
- After applying the magnetic field, the bias of z vorticity disappears and the bubble is seen to rise rectilinearly

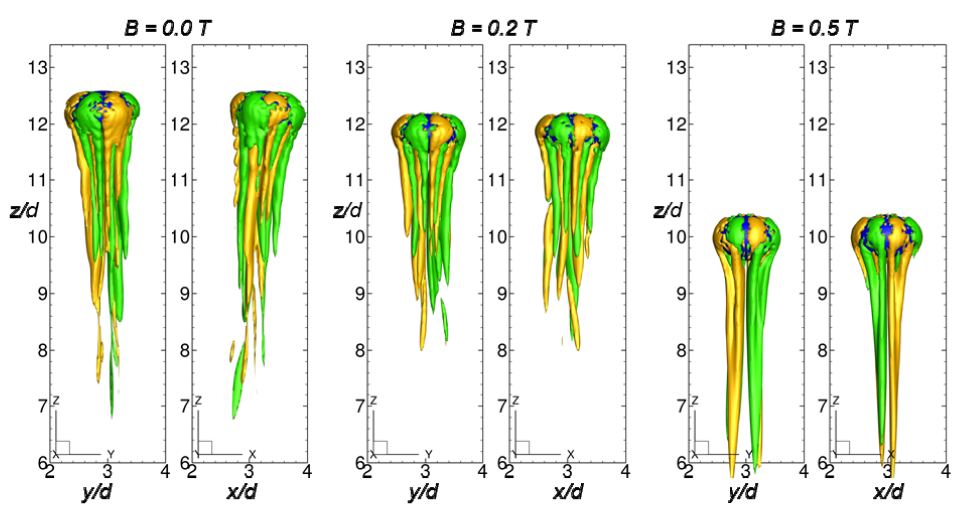

Wake behind the 7mm Bubble (Z Vorticity)

- Front and side views, isosurfaces of $\Omega^*_z = \pm 1$ at t=0.24s for the 7mm bubble
- Alternating pattern of Ω^*_z is seen
- With a magnetic field of 0.2 T, it is seen more clearly that the isosurfaces are elongated in the magnetic field direction (x direction).

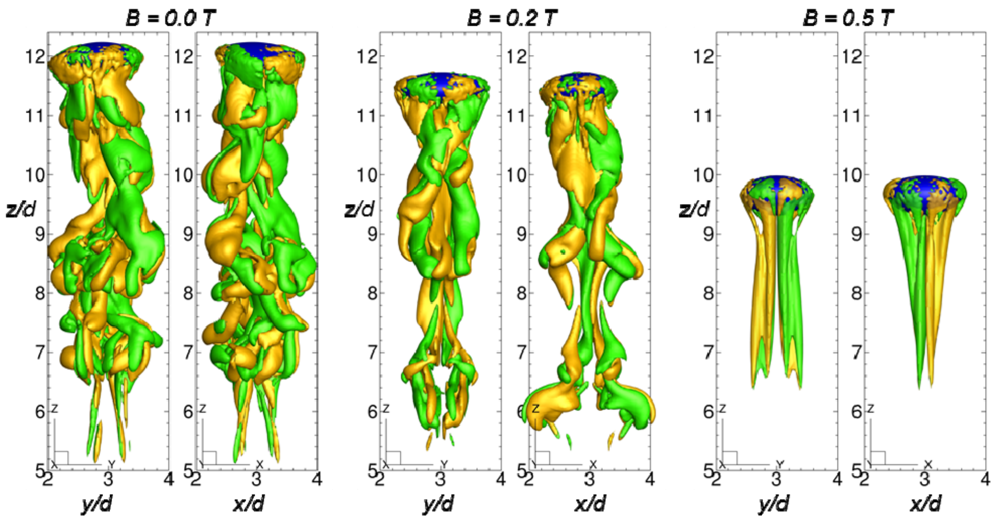

Bubble Rise Velocity

- d = 3mm, rise velocity curves are smooth and non-oscillatory
- d = 7mm, B = 0 and 0.2 T, rise velocity curve is oscillatory after the initial rise; B = 0.5 T, a steady rise velocity curve is seen
- With EMBr, bubble rises smoother and slower

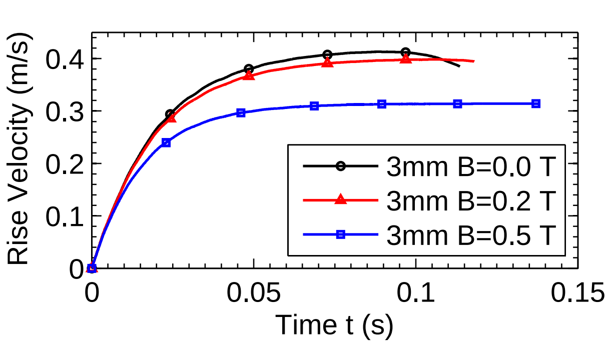

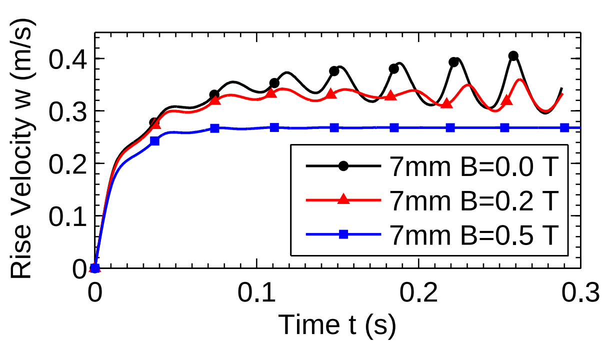

Shape of the 3mm Bubble with B = 0 T and B = 0.2 T

- d = 3mm, top and side views of the bubble
- With no EBMr, rise velocity decreases after t>0.1s, due to bubble transverse motion

Bubble Rise velocity and **Top views** (x-y plane) of the 3 mm bubble

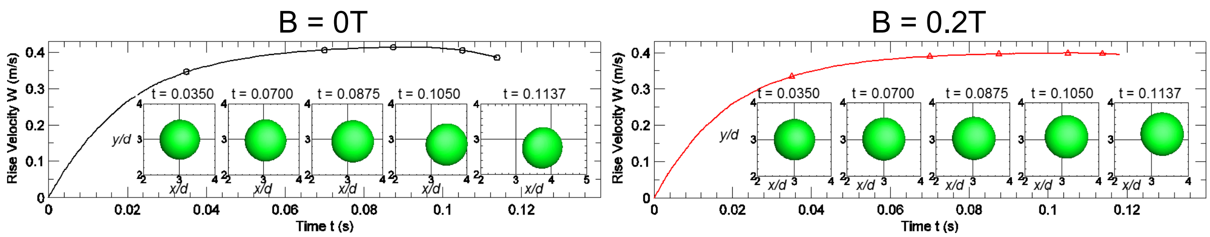

Side views (x-z plane) of the 3 mm bubble

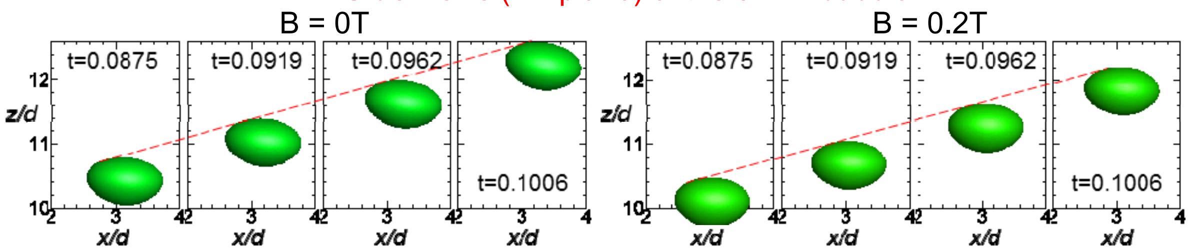

Shape of the 3mm Bubble with B = 0.5 T

- d = 3mm, B = 0.5T: top, side and front view of bubble at t = 0.1225s
- No significant rotation of the bubble is observed
- Ellipsoidal bubble, slightly elongated in magnetic field direction

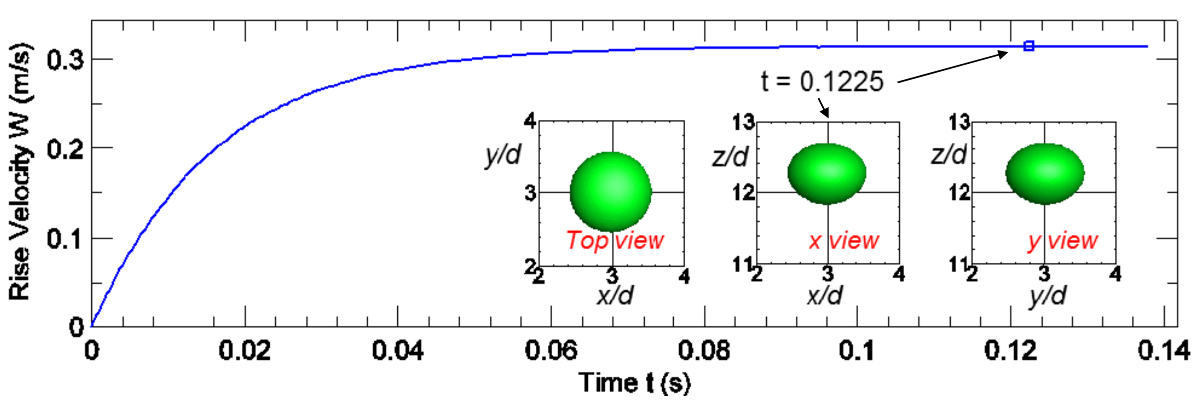

Shape of the 7mm Bubble At initial stage t<0.05s

- In initial stage the bubble rose with the same velocity for all B
- large deformation between t=0 to 0.03s:
  - changes from a sphere to a mushroom-head-like shape at t=0.02004s
  - then deforms into a squeezed (in z direction) ellipsoidal at t=0.03340s
- Viscous and surface tension effects dominate early deformation stage

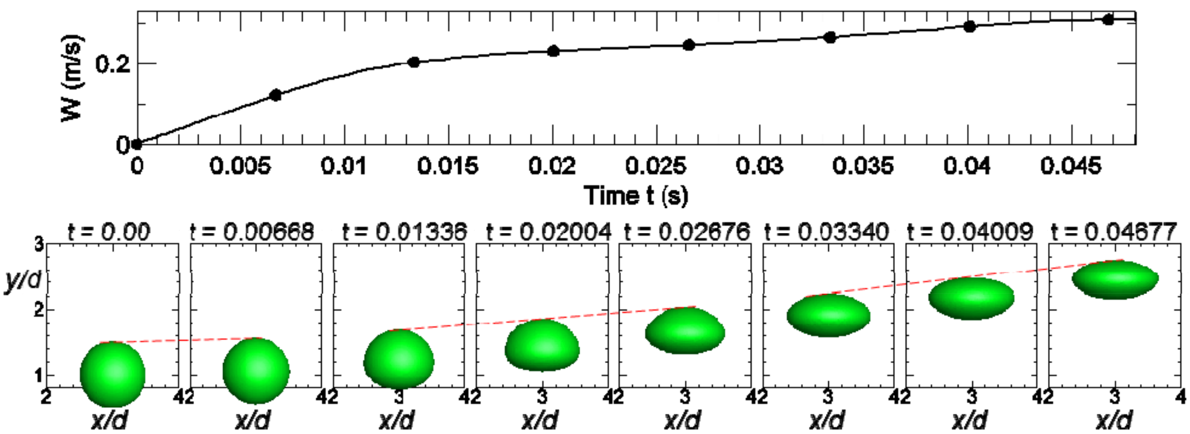

Top View of 7mm Bubble with B = 0 T and B = 0.2 T

- First symmetrical deformation and forms an ellipsoidal disk at t=0.053s
- Number of cells in largest bubble cross section are given in each sub figure
- Rise velocity not simply proportional to largest cross section area

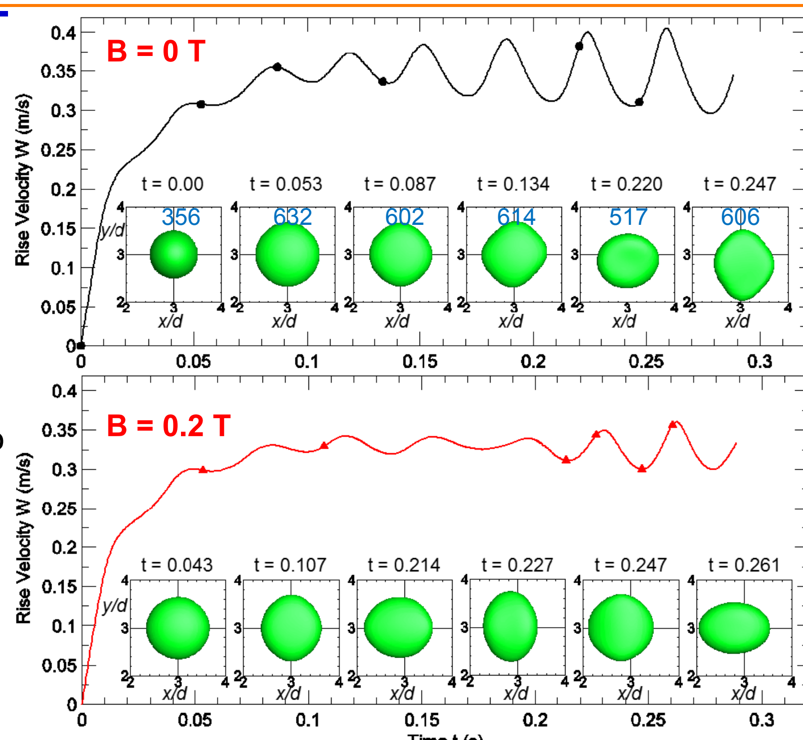

Front View of 7mm Bubble with B = 0 T and B = 0.2 T

- 7mm bubble: Larger deformation
- With B = 0.2 T, bubble rise slower, but bubble shape still oscillate

Front View of the 7mm bubble, **B = 0 T**

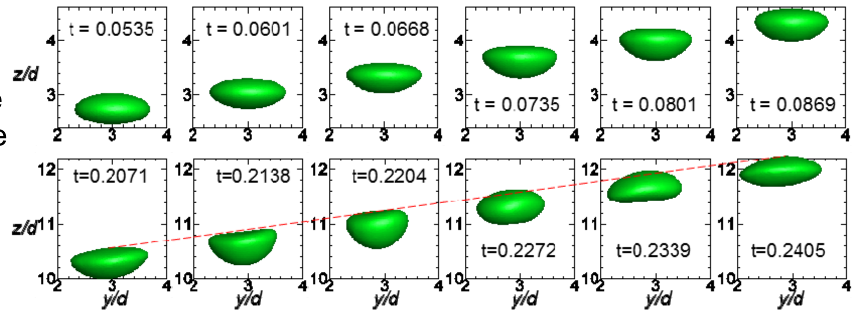

Front View of the 7mm bubble, **B = 0.2 T**

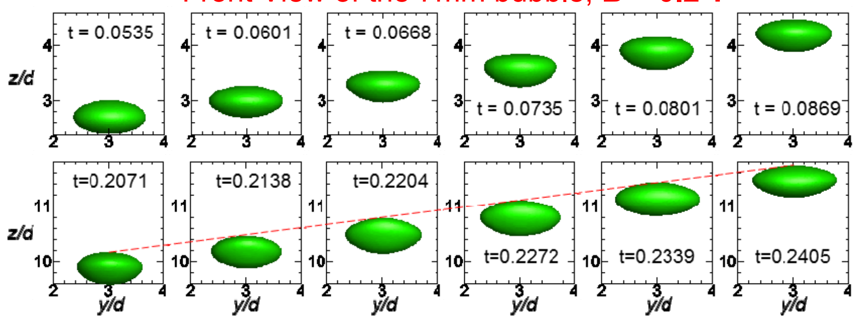

Top, Front and Side View of 7mm Bubble at B = 0.5 T

- More stable rise of the bubble
- No time dependent variation of bubble shape is seen, largest cross section has 526 cells
- Bubble is slightly elongated in the direction of magnetic field (1.24d along x and 1.16d along y)
- Bubble oscillations are suppressed and the steady rise velocity is reduced to 75% of that with B = 0

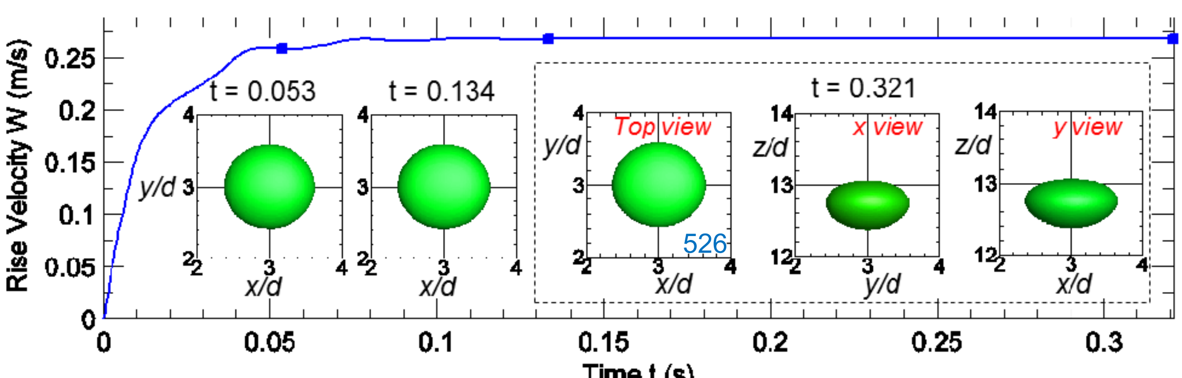

Predicted Bubble Reynolds Number and Argon Bubble Shape on Grace Diagram

- Increasing EMBr leads to smaller bubble Reynolds number Re_τ
- Increasing EMBr, 7mm bubble becomes less wobbling and bubble shape is more close to oblate ellipsoid

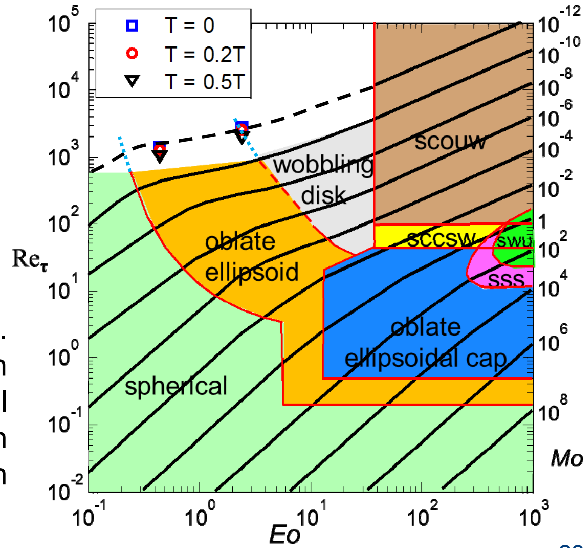

Eo vs. predicted Re_τ on Grace diagram. Bubble shape: scouw - spherical cap with open unsteady wake; sccsw - spherical cap with closed steady wake; swu - with wavy unsteady skirt; sss – with smooth steady skirt [5, 6]

Velocity close to 7mm Bubble

- w velocity contour close to bubble at t=0.0668s for different B
- Recirculation pattern at the boundary of the bubble
- Comparing B = 0 and B = 0.2T, the maximum vertical velocity w at the bottom of the bubble is reduced from 0.42m/s to 0.34m/s
- With B = 0.5T, bubble becomes thicker and less squeezed in z

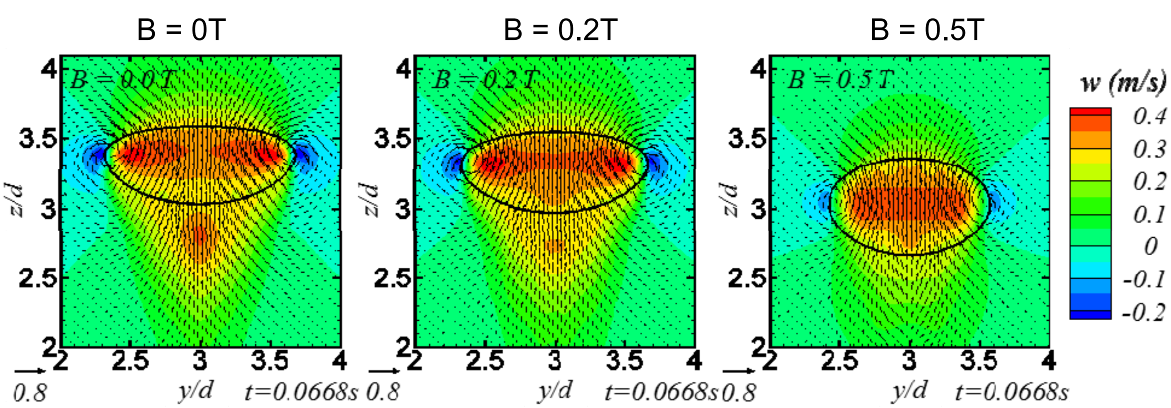

Lorentz Force in Y-Z plane

- Contour of Lorentz Force (dimensionless), d=7 mm, t=0.0668s, in y-z plane
- Top half of the bubble: force points inside of the bubble, tries to squeeze the bubble along y and z directions.
- Bottom half of the bubble: the y component of the F_L is positive on right side but negative on left side → pull liquid away from bubble
- z component of the F_L tends to accelerate the flow at the side of the bubble (as a resistance force to diminish the recirculation and decelerate the downward motion of the liquid near the sides of the bubble).

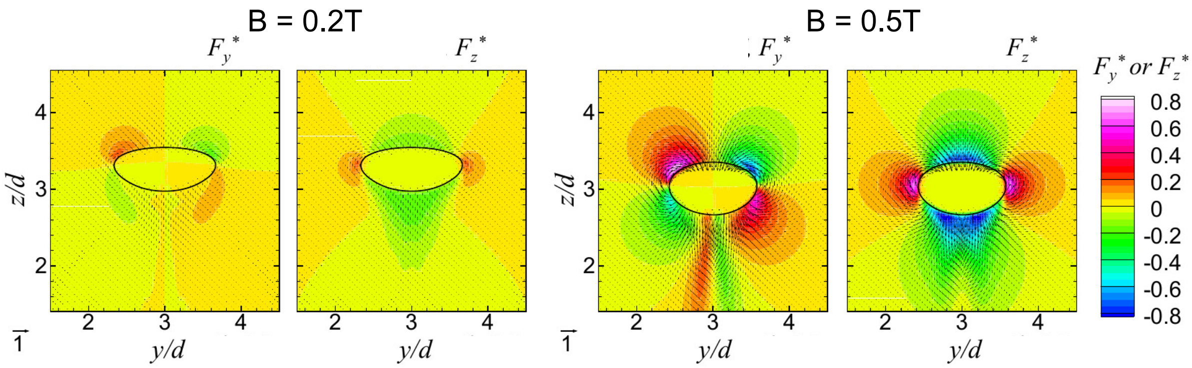

Isosurfaces of Constant Lorentz Force

- d = 7 mm, B = 0.5, t=0.23s
- Isosurface of constant y and z components of dimensionless F_L

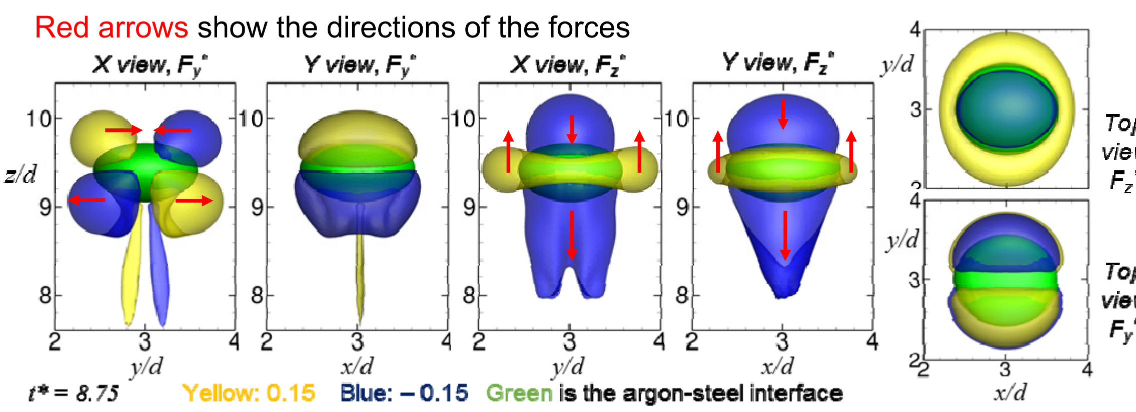

Note: * means dimension less veriables

Lorentz Force and Bubble Shape

- 1/4 of the bubble and the isosurfaces of constant F_y^*, Lorentz force vectors in the quarter planes, t= 0.2339s, d=7mm, B=0.5T
- Distribution of F_y^* in two x-y planes
  - z/d = 9.2 cuts bottom half of the bubble, Lorentz force shows pulling along y
  - z/d = 9.6 cuts top half of the bubble, shows compression of the liquid along y

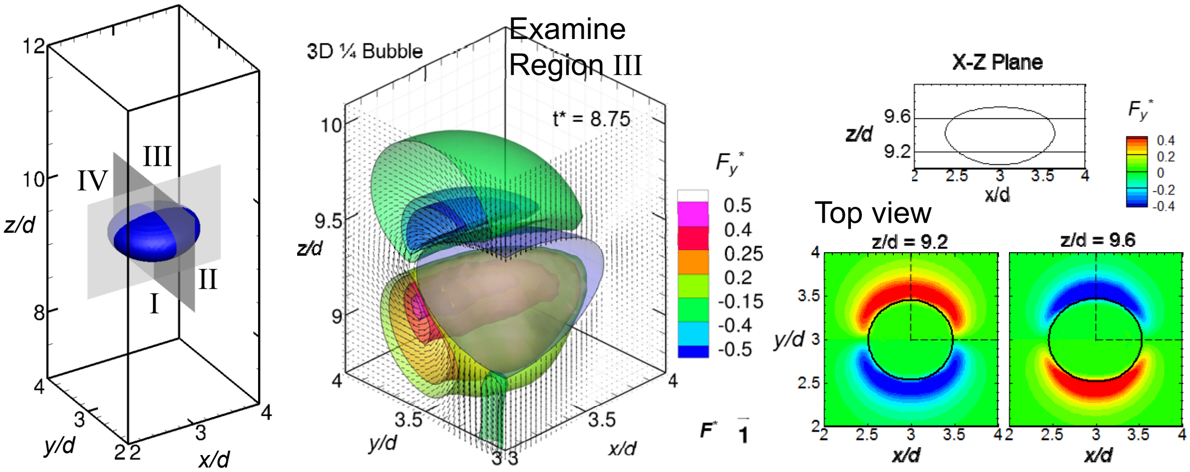

Conclusions

- Small bubbles remain almost spherical.
- Without a magnetic field, oscillating rise velocity of larger bubbles is closely related to the variation of bubble shape;
- EMBr makes bubble rise smoother, slower, and straighter;
- Large (7mm) bubbles experience alternating elongation with weak magnetic field (B = 0 and B = 0.2 T);
- All bubbles elongate along the magnetic field direction with strong magnetic field (B=0.5T);
- Wake structures behind bubble are lessened by magnetic field.

Future Work

Implement the results of this single-bubble VOF model study into the multiphase Lagrangian particle model used to study continuous casting with EMBr.

- Test a single bubble rise under EMBr using two-way coupled Lagrangian method, and compare relative rising velocity ($v_{fluid} – v_{bubble}$) with VOF model results
- Determine additional forces or modifications to the drag laws to add into the particle motion equations of the Lagrangian model

Acknowledgment

- Continuous Casting Consortium Members (ABB, AK Steel, ArcelorMittal, Baosteel, JFE Steel Corp., Magnesita Refractories, Nippon Steel and Sumitomo Metal Corp., Nucor Steel, Postech/ Posco, SSAB, ANSYS/ Fluent)
- National Science Foundation Grant CMMI-11-30882
- Blue Waters / National Center for Supercomputing Applications (NCSA) at UIUC
- NVIDIA for providing the GPU cards through the NVIDIA Professor Partnership program

References

1. L. Zhang, J. Aoki, and B. G. Thomas, "Inclusion removal by bubble flotation in a continuous casting mold," Metallurgical and Materials transactions B **37**, 361–379 (2006).

2. K. Jin, P. Kumar, S. P. Vanka and B. G. Thomas "Rise of a Argon Bubble in Liquid Steel in the Presence of a Transverse Magnetic Field," manuscript submitted to *Physics of Fluids*

3. Z. Wang and A. Y. Tong, "Deformation and oscillations of a single gas bubble rising in a narrow vertical tube," in *ASME 4th International Conference on Nanochannels, Microchannels, and Minichannels* (American Society of Mechanical Engineers, 2006) pp. 1195–1202.

4. Z. Wang and A. Y. Tong, "Deformation and oscillations of a single gas bubble rising in a narrow vertical tube," International Journal of Thermal Sciences **47**, 221–228 (2008).

5. J. Grace, "Shapes and velocities of bubbles rising in infinite liquids," Trans. Inst. Chem. Eng. **51**, 116–120 (1973).

6. D. Bhaga and M. Weber, "Bubbles in viscous liquids: shapes, wakes and velocities," Journal of Fluid Mechanics **105**, 61–85 (1981).